

Time-Varying Beam Quality Factor and Mode Evolution in TEA CO₂ Laser Pulses

F. Encinas-Sanz, J. Serna, C. Martínez, R. Martínez-Herrero, and P. M. Mejías

Abstract—The time evolution of the transversal modes in a TEA CO₂ laser cavity has been investigated from the analysis of the time-varying beam quality factor M^2 of the emitted pulses. The experiments reveal a significant change in this parameter during the pulse evolution, which can be translated into an evolution of the modes of the laser cavity to reach a nearly stationary behavior. Attention is focused on both the appearance of a particular mode and the duration of its growing process.

Index Terms—Beam quality, laser modes, TEA CO₂ lasers.

I. INTRODUCTION

IN GENERAL, the spatial profile of a laser pulse cannot be expected *a priori* to remain constant during the pulse evolution [1]–[4]. To characterize this evolution in a rigorous way, time-resolved spatial parameters were recently introduced [5], [6] on the basis of the intensity moments formalism [7]–[11]. Under certain conditions which are often met in practice, as occurs for the pulses considered in this paper, it was shown that the second-order moments that characterize the instantaneous field profile (time-slice approach) at the input and output planes of an optical system are related by the same propagation law used to describe the propagation of nonvarying (time-integrated) moments.

In this paper we are interested in the time evolution of the transversal modes in the laser cavity. More specifically, attention is focused on both the instant (within the pulse length) in which the presence of a particular mode begins to be significant and the time interval during which such mode grows to reach a quasi-stationary spatial behavior. As we will see in the following, this kind of information can be inferred from both the experimental analysis of the time-varying M^2 parameter of the pulse and the transversal mode beating measurements. Thus, in Section II, we describe the experimental setup in detail. In Section III, the experimental results concerning the evolution of the beam quality factor M^2 during the pulse are presented, and we discuss a number of conclusions about mode appearance and evolution in Section IV.

II. EXPERIMENTAL SETUP

We consider in this work the pulses emitted by a TEA CO₂ laser device, with the presence of nitrogen in the gas mixture.

Manuscript received March 9, 1998; revised June 11, 1998. This work was supported by the Comisión Interministerial de Ciencia y Tecnología of Spain under Project TAP96-2333-E within the framework of EU-1269 Eureka Project.

The authors are with the Departamento de Óptica, Facultad de Ciencias Físicas, Universidad Complutense, 28040 Madrid, Spain.

Publisher Item Identifier S 0018-9197(98)07163-2.

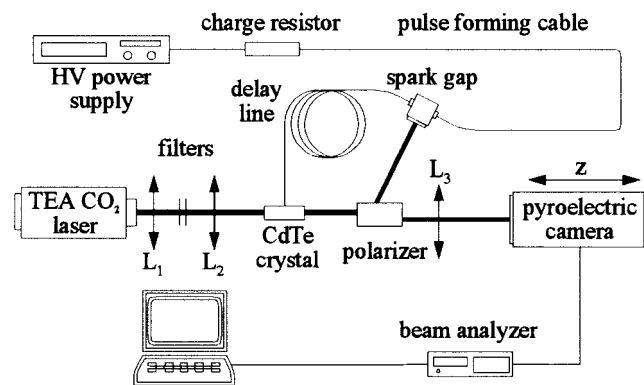


Fig. 1. Experimental setup for the measurement of the M^2 factor.

We have also installed an intracavity diaphragm to reduce the Fresnel number. The laser cavity is a half-symmetric resonator in which the distance between the curved mirror (radius of curvature 10 m) and the planar output mirror is 112 cm [12]. An intracavity Brewster plate has been introduced to obtain a linearly polarized beam. The beam width has been determined at different planes for time slices whose thickness (10 ns) is typically much shorter than the complete pulse duration ($\sim 2 \mu\text{s}$). By repeating this series of measurements during the pulse evolution at time intervals of tens of nanoseconds, we can get the beam quality factor resolved in time.

The experimental setup is shown in Fig. 1. The ensemble pyroelectric camera (Spiricon PYROCAM I), laser beam analyzer, and computer provides the (squared) beam widths averaged during each time slice. To cut such time slices an electrooptical switching device formed by a CdTe crystal and a polarizer was used, with the transmission axis of the polarizer perpendicular to the polarization of the beam emerging from the laser cavity. A high-voltage pulse (8.48 kV) produces a transverse Pockels effect in the CdTe crystal, which turns 90° the polarization of the linearly polarized laser beam. As a result, the beam is transmitted by the crossed polarizer as long as the high-voltage pulse lasts. The system is fired by the polarizer itself, using a spark gap that collects the rejected beam at the polarizer. The duration of the electronic pulse is given by the length of the coaxial forming cable that links the spark gap and the high-voltage charge resistor, and the relative position of the time slice within the laser pulse is controlled by the length of the delay cable between the spark gap and the switching device. A reference time for each slice was measured by splitting the beam before the electrooptical device in such a way that the complete pulse is collected by a fast photodetector (photon drag, 1-ns rise time), and the

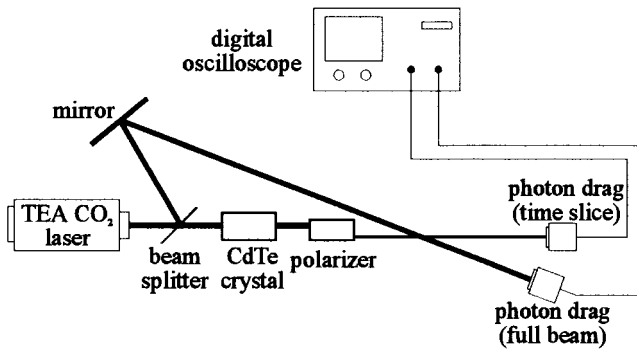


Fig. 2. Experimental arrangement for measuring the reference time for each time slice within the pulse duration.

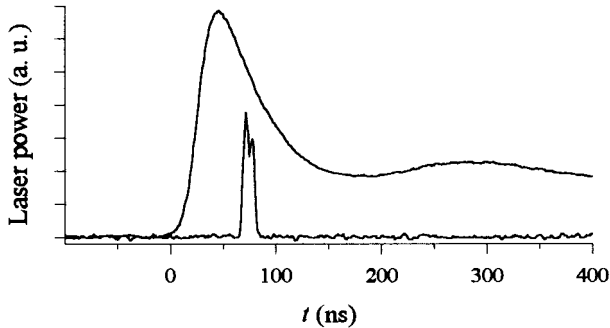


Fig. 3. Illustration of the relative position of a time slice ($t_0 \sim 75$ ns) using the experimental setup shown in Fig. 2. Mode beating has been filtered out in the full pulse.

chopped pulse (time slice) is registered by another photon drag detector after crossing the polarizer (see Fig. 2). The relative position of a time slice with respect to the pulse is illustrated in Fig. 3 for a delay of $t_0 \sim 75$ ns measured from the beginning of the pulse. A variable number of CaF_2 filters have been used in the setup to reduce the total irradiance and to take advantage of the dynamic range of the camera. The filtering mechanism is absorption, not scattering. Special care was taken to check that the filters do not distort the beam and do not change the beam size.

The polarizer is based on two successive reflections at Brewster's angle and introduces no distortion on the spatial structure of the beam profile. It also provides a secondary beam to fire the spark gap, as was previously mentioned.

The telescopic system formed by lenses L_1 and L_2 avoids hard edge diffraction at the electrooptical crystal aperture by reducing the beam size through the crystal and maintains the energy density below the threshold damage level of the material. In Fig. 1, the paraxial focal lengths of L_1 and L_2 are, respectively, $f_1 = 25$ cm and $f_2 = 12.5$ cm. A third lens L_3 ($f_3 = 50$ cm) is used to generate a waist at the measurement region.

III. MEASUREMENT OF THE TIME-RESOLVED M^2 FACTOR

Using the above experimental arrangement, we have measured the (squared) beam size $\langle x^2 \rangle$ along, say, the x axis, transverse to the propagation direction of the beam, z , for different time positions t_0 of the time slice during the pulse

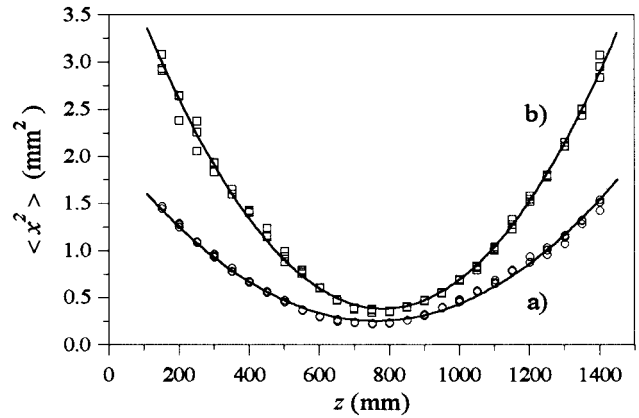


Fig. 4. Squared beam width (x^2) versus propagation distance z measured from lens L_3 for (a) $t_0 = 30$ ns and (b) $t_0 = 525$ ns after the leading edge of the pulse. Intracavity aperture diameter $d = 10$ mm.

evolution. Note that the measured second-order moment $\langle x^2 \rangle$ is expressed in terms of the field amplitude f at plane z_0 as follows:

$$\langle x^2 \rangle(z_0, t_0) = \frac{1}{H_{t_0}} \int_{t_0}^{t_0 + \Delta t} dt \int x^2 |f|^2 dx dy \quad (1)$$

where $H_{t_0} = \int_{t_0}^{t_0 + \Delta t} dt \int |f|^2 dx dy$ is the total energy of the time slice at t_0 , and $\Delta t \simeq 10$ ns is the FWHM temporal thickness of each time slice. The integration in the t variable indicates that, strictly speaking, we do not determine the instantaneous value of the beam size, but an average over a very short time interval Δt . The measurements were performed at various distances after the lens L_3 and three pulses were registered at each location z_0 .

Within the intensity moment's formalism, one can define the time-resolved bidimensional beam quality factor M^2 as follows [9]:

$$M^2 = \sqrt{4k^2 \langle x^2 \rangle_w \langle \theta^2 \rangle} \quad (2)$$

where $k = 2\pi/\lambda$ ($\lambda = 10.6 \mu\text{m}$), the subscript w refers to the beam waist plane and $\langle \theta^2 \rangle$ denotes the far-field divergence associated with the x variable (again integrated over the time interval Δt). The values of $\langle x^2 \rangle$ measured versus propagation distance z_0 can be fitted to a parabola, and from the parameters of the fitting parabola the value of M^2 is easily inferred. Fig. 4 illustrates such a fitting parabola for $t_0 = 30$ ns and $t_0 = 525$ ns after the pulse leading edge. To increase the accuracy in the measurement of $\langle x^2 \rangle$, a numerical circular aperture was placed around the beam and no camera data were computed beyond that window in the calculations. Note that the smoothness of the curves plotted in Fig. 4 confirms that the CaF_2 filters have no influence on the beam width.

Two series of measurements have been performed, which correspond to the values of the intracavity aperture $d = 8$ mm and $d = 10$ mm. For the first case, $d = 8$ mm, M^2 remains essentially constant throughout the pulse, with a value close to $M^2 = 1.1$. In the second case, $d = 10$ mm, the s -shaped curve that gives the measured evolution of M^2 [Fig. 5(a)] exhibits three different parts: a first region at the beginning of the pulse, $t_0 < 100$ ns, in which M^2 is nearly 1 (~ 1.1); a second region,

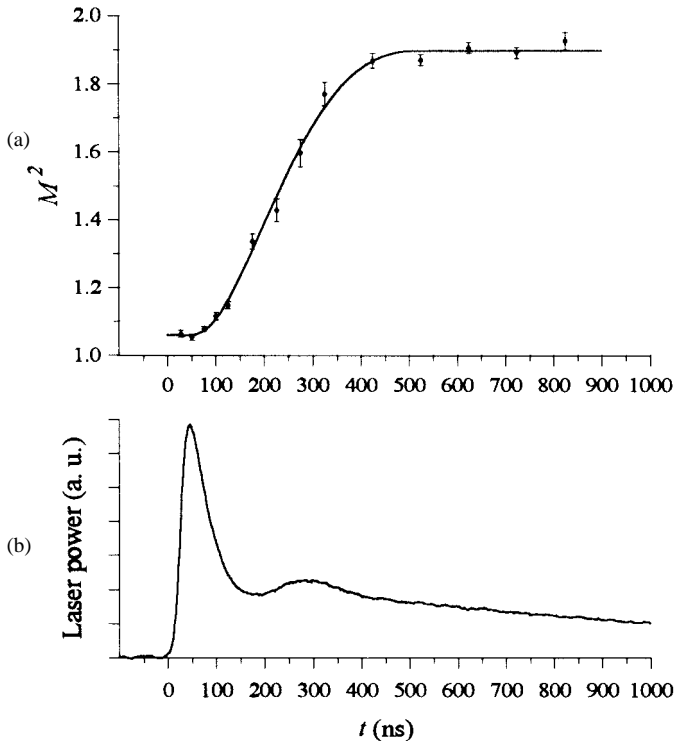


Fig. 5. (a) Evolution of the beam quality factor M^2 along the pulse duration ($d = 10$ mm). (b) Pulse power (in arbitrary units) plotted for time reference.

$100 \text{ ns} < t_0 < 500 \text{ ns}$, in which M^2 increases to reach a value of about 1.9; and finally, a third region, $t_0 > 500 \text{ ns}$, where M^2 is nearly constant. This figure also shows the standard deviation of these measurements, calculated from the least-squares fitting of the experimental points. Fig. 5(b) plots the pulse power for time reference. It should be noted that the energy content of the pulse in the time interval $0 < t_0 < 60 \text{ ns}$ (which includes the pulse peak) is much smaller than the total energy throughout the rest of the pulse.

IV. DISCUSSION

The above experimental results allow one to obtain a number of conclusions about the dynamical behavior of the cavity modes. Here we associate the term “modes” with defined spatial structures of the laser field, which resonate within the *loaded* cavity. The existence of different modes would then announce the presence of different transversal mode resonance frequencies.

Note first that there is a 300–400-ns delay between the moment the pumping discharge begins and the moment when the pulse is strong enough to be detected by a linear photon drag detector over the noise level [13]. Consequently, it is reasonable to consider that the radiation, starting from an incoherent low-level signal, has undergone a fairly large number of round trips (~ 40 – 50 , approximately) before the leading edge of the pulse begins to be detected.

When the diameter of the intracavity diaphragm is $d = 8$ mm, the measurement of the so-called mode beats, generated by heterodyne interference effects at different frequencies between the modes, shows that, in this case, there is only one mode [12] (diffraction losses are strong enough to prevent the

appearance of higher order modes). Moreover, the experiment shows that the beam quality factor is nearly one and remains constant along the pulse. Therefore, we conclude that for $d = 8$ mm, the beam profile quickly reaches a nearly stationary Gaussian-like spatial structure, which is maintained during the pulse duration.

The evolution of the spatial behavior of the pulse is completely different when $d = 10$ mm [Fig. 5(a)]. In this case, diffraction losses are reduced and higher order modes can grow after successive round trips. Since a higher order mode requires supplementary time to grow, it can be expected that the spatial behavior at the beginning of the pulse is similar to that observed in the previous case ($d = 8$ mm). This is confirmed by the experiments, since the beam quality factors take the same values ($M^2 \sim 1$) in both cases and the spatial structure is nearly Gaussian again. However, for times greater than, say, 100 ns, the beam quality factor begins to deteriorate and the structure of the beam profile changes. The existence of only two modes in this region of the pulse ($t_0 > 100 \text{ ns}$) has been observed from the mode beating between transversal mode frequencies, associated with different spatial structures [12]. The M^2 parameter increases smoothly as the second mode grows until it reaches a value of about 1.9. After a large enough number of round trips (60–70 from the leading edge of the pulse), it reaches a nearly stationary spatial behavior and the beam profile remains constant [third region of the curve in Fig. 5(a)].

Fig. 5(a) and (b) also shows that the second mode begins to be significant after the gain switch peak of the pulse. This explains why mode beat experiments [12] show the presence of only one mode when $d = 10$ mm and no nitrogen is present in the gas mixture; in such a case, only the gain switch pulse is formed, lasting ~ 90 ns, so that there is not enough time for the second mode to grow in amplitude. This confirms the validity of the above analysis about the evolution of the modes.

In summary, we can say that the time-varying beam quality factor of a pulse, together with transversal mode beating measurements, provides a useful tool to investigate the evolution of the modes in a TEA CO₂ laser cavity.

REFERENCES

- [1] A. Caprara and G. C. Reali, “Time-resolved M^2 of nanosecond pulses from a Q -switched variable-reflectivity-mirror Nd:YAG laser,” *Opt. Lett.*, vol. 17, pp. 414–416, 1992.
- [2] T. Omatsu and K. Kuroda, “Time-resolved measurements of spatial coherence of a copper vapor laser using a reversal shearing interferometer,” *Opt. Commun.*, vol. 87, pp. 278–286, 1992.
- [3] J. J. Chang, “Time-resolved beam-quality characterization of copper vapor lasers with unstable resonators,” *Appl. Opt.*, vol. 33, pp. 2255–2265, 1994.
- [4] M. R. Perrone, C. Palma, V. Biagini, A. Piegari, D. Flori, and S. Scaglione, “Theoretical and experimental determination of single round-trip beam parameters in a XeCl laser,” *J. Opt. Soc. Amer. A*, vol. 12, pp. 991–998, 1995.
- [5] P. M. Mejías and R. Martínez-Herrero, “Time-resolved spatial parametric characterization of pulsed light beams,” *Opt. Lett.*, vol. 20, pp. 660–662, 1995.
- [6] M. Morin, M. Lebesque, A. Mailloux, and P. Galarneau, “Moment characterization of the position stability of laser beams,” in *Proc. Soc. Photo-Opt. Instrum. Eng.*, 1996, vol. 2870, pp. 206–215.
- [7] S. Lavi, R. Prochaska, and E. Keren, “Generalized beam parameters and transformation laws for partially coherent light,” *Appl. Opt.*, vol. 27, pp. 3696–3703, 1988.

- [8] M. J. Bastiaans, "Propagation laws for the second-order moments of the Wigner distribution function in first-order optical systems," *Optik*, vol. 82, pp. 173–181, 1989.
- [9] A. E. Siegman, "New developments in laser resonators," in *Proc. Soc. Photo-Opt. Instrum. Eng.*, 1990, vol. 1224, pp. 2–14.
- [10] J. Serna, R. Martínez-Herrero, and P. M. Mejías, "Parametric characterization of general partially coherent beams propagating through ABCD optical systems," *J. Opt. Soc. Amer. A*, vol. 8, pp. 1094–1098, 1991.
- [11] H. Weber, "Propagation of higher-order intensity moments in quadratic-index media," *Opt. Quantum Electron.*, vol. 24, pp. 1027–1049, 1992.
- [12] C. Martínez, F. Encinas-Sanz, J. Serna, P. M. Mejías, and R. Martínez-Herrero, "On the parametric characterization of the transversal spatial structure of laser pulses," *Opt. Commun.*, vol. 139, pp. 299–305, 1997.
- [13] F. Encinas-Sanz and J. M. Guerra, "The peaking capacitor in an incomplete corona surface discharge preionized TEA CO₂ laser," *IEEE J. Quantum Electron.*, vol. 27, pp. 891–894, 1991.
- J. Serna**, photograph and biography not available at the time of publication.
- C. Martínez**, photograph and biography not available at the time of publication.
- R. Martínez-Herrero**, photograph and biography not available at the time of publication.

F. Encinas-Sanz, photograph and biography not available at the time of publication.

P. M. Mejías, photograph and biography not available at the time of publication.